


Cite this: *RSC Adv.*, 2022, 12, 25852

# Detection and discrimination of sulfur dioxide using a colorimetric sensor array†

Chaoqiang Ding,<sup>a</sup> Yan Ren,<sup>a</sup> Xinyang Liu,<sup>a</sup> Jingjing Zeng,<sup>a</sup> Xinping Yu,<sup>a</sup> Daxiang Zhou<sup>a</sup> and Yanjie Li<sup>ID</sup> \*<sup>ab</sup>

Discrimination and detection of sulfur dioxide residues in foods using a simple colorimetric array have been achieved. The difference maps before and after the reaction showed that the specific color fingerprint was related to the amount of sulfur dioxide. The results of principal component analysis (PCA), hierarchical clustering analysis (HCA) and linear discriminant analysis (LDA) demonstrated that the as-fabricated colorimetric sensor array have good performance for the discrimination of sulfur dioxide and other interferents, as well as different concentrations of sulfur dioxide. Moreover, the array has been successfully applied to determine the concentration of sulfur dioxide residues in real samples and revealed good accuracy, precision and repeatability.

Received 10th July 2022  
Accepted 3rd September 2022

DOI: 10.1039/d2ra04251g

rsc.li/rsc-advances

## 1. Introduction

Sulfur dioxide in food mainly comes from permissible, legal, direct addition and sulfur-fumigation. Sulfur-fumigation, a process of Traditional Chinese Medicine (TCM) to prolong the storage period, mainly protects herbs from insects and molds.<sup>1</sup> In addition, sulfur-fumigation can also improve the appearance of TCM or foods through a whitening effect. Excessive sulfur dioxide residues lead to potential health risks through excessive or irregular use of sulfur-fumigation. Studies that indicate the excessive residues of sulfur dioxide not only induce respiratory system damage,<sup>2</sup> but also irreversible damage to reproductive system,<sup>3</sup> digestive system,<sup>4</sup> circulatory system,<sup>5</sup> nervous system<sup>6</sup> and immune system,<sup>7</sup> and even life-threatening.<sup>8</sup> More significantly, residual sulfur dioxide is prone to chemical reactions with ketones and hydroxyl groups in some herbs and foods, resulting in the loss of active ingredients.<sup>9,10</sup>

As consumers pay more and more attention to food and drug safety, there are more and more calls to cancel sulfur-fumigation. Since the Chinese Pharmacopeia 2005 version, sulfur-fumigation had been prohibited for all herbals during storage and processing.<sup>11</sup> Further, the residue limit standard for sulfur dioxide was firstly stipulated for herbals and tablets in China Pharmacopoeia 2010 edition (2nd supplement).<sup>12</sup> Likewise, according to GB

5009.34-2016 Chinese National Food Safety Standard-Determination of sulfur dioxide in foodstuffs, sulfur-fumigation was currently only permitted for several foods, and the maximum residue limit (in terms of residual sulfur dioxide) was clearly stated.<sup>13</sup> However, the attractive appearance of raw herbs is easier to close the deal and bring additional benefits, and improper use, abuse and even illegal use of sulfur-fumigation are still not uncommon. In particular, in addition to TCM, it has been reported that the sulfur-fumigation process has been illegally used in many foods and food ingredients (*e.g.*, star anise, pepper, wolfberry, ginger, fungus and tremella).<sup>10,14</sup>

Currently, the pharmacopoeias and food laws of many countries and regions have stipulated the limits of sulfur dioxide residues and recommended a variety of detection methods for sulfur dioxide residue, such as spectrophotometry,<sup>15</sup> acid-base titration,<sup>16</sup> fluorescence method,<sup>17,18</sup> gas chromatography-mass spectrometry,<sup>19</sup> high-performance liquid chromatography,<sup>20</sup> electrochemical analysis,<sup>21</sup> enzyme-linked immunosorbent assays<sup>22</sup> and Fourier-transform infrared spectroscopy.<sup>23</sup> Although the above-mentioned means exhibit high sensitivity and selectivity, their popularization and application are generally limited by high costs, unfriendly portability, complex sample pretreatment, and specialized technical training in some developing countries and regions.

Besides that, on-site detection has always been a difficult problem and challenge for the above conventional analysis methods. Therefore, it is necessary to develop a simple, sensitive and easy on-site detection approach for sulfur dioxide residues.

Based on the principle of bionics,<sup>24</sup> a typical colorimetric sensor array is designed as follows: a series of specific chromatic reactions are selected or designed to form a cross-responsive colorimetric array, and the detection of the analytes is achieved through the corresponding color fingerprints. At

<sup>a</sup>College of Biology and Food Engineering, Chongqing Three Gorges University, Wanzhou, Chongqing 404100, P. R. China. Fax: +86 23 5810 2522; Tel: +86 23 5810 2522

<sup>b</sup>Engineering Technology Research Center for the Development and Utilization of Characteristic Biological Resources in Northeast Chongqing, Chongqing Three Gorges University, Wanzhou, Chongqing 404100, P. R. China. E-mail: 20060016@sanxiao.edu.cn

† Electronic supplementary information (ESI) available. See <https://doi.org/10.1039/d2ra04251g>


present, some studies reported that the colorimetric sensor array has been successfully used for the detection of pesticide residue and the analysis of sensory quality in food.<sup>25–29</sup>

In this work, an improvised and inexpensive colorimetric sensor array for detecting sulfur dioxide was developed on the base of six specific and high-sensitive color reactions. The assessment of availability and practicability of the colorimetric array was reached through principal component analysis (PCA), hierarchical cluster analysis (HCA) and linear discriminant analysis (LDA). And the determination of sulfur dioxide content in real samples was achieved by the method of fitting curve.

## 2. Experimental details

### 2.1 Reagents and materials

All chemicals from commercial sources are of analytical grade and used as received without further purification unless otherwise specified. Sulfur dioxide detection kits (in view of hydrochloric *para*-rosaniline method) were purchased from Ruixin Technological Instrument Co., Ltd (Shanghai, China). Sodium sulfite, brilliant green, malachite green, basic fuchsin, *O*-phthalaldehyde, ammonium acetate, 1,10-phenanthroline, ferric chloride, hexadecyl trimethyl ammonium bromide (CTAB), phosphate-buffered saline (PBS), borax, sodium acetate, acetic acid, sodium hydroxide and absolute alcohol were provided by Aladdin Biochemical Technology Co., Ltd (Shanghai, China). Deionized water was used throughout this work.

1.0 mL brilliant green ( $80 \mu\text{g mL}^{-1}$ ) and malachite green ( $46.34 \mu\text{g mL}^{-1}$ ) were prepared separately by directly dissolving in PBS (10 mM, pH 7.0). 0.5 mL basic fuchsin ( $55 \mu\text{g mL}^{-1}$ ) was diluted to 2.0 mL with borax buffer (1.47 mM, pH 9.16). 0.5 mL *o*-phthalaldehyde ( $1.34 \times 10^{-2} \mu\text{g mL}^{-1}$ ) and 0.5 mL ammonium acetate ( $3.85 \times 10^{-3} \mu\text{g mL}^{-1}$ ) were mixed and diluted to 2.0 mL with potassium dihydrogen phosphate buffer (4 mM, pH 6.6). A mixture of 0.3 mL 1,10-phenanthroline ( $3.6 \times 10^{-3} \mu\text{g mL}^{-1}$ ), 0.05 mL ferric chloride ( $3.24 \times 10^{-3} \mu\text{g mL}^{-1}$ ) and 0.5 mL CTAB (0.5%) was diluted to 2.0 mL with sodium acetate anhydrous solution (0.5 mM, pH 5.5). The reagents of the sulfur dioxide detection kit were dissolved in PBS (10 mM, pH 7.0) according to the kit instructions. Sodium sulfite was dissolved in deionized water ( $5.0 \text{ g L}^{-1}$ ) before use and immediately mixed with formaldehyde (1% final concentration). Note that all the reagents mentioned above were freshly prepared before the experiments to minimize their potential effects of hydrolysis.

*Fritillaria cirrhosa* D. Don is a common edible and medicinal plant in many countries and regions. *Fritillaria* samples without sulfur dioxide residue were purchased from a local traditional Chinese medicine (TCM) pharmacy in Chongqing, China, and analyzed by iodine titration (according to Chinese National Standard GB 5009.34-2016) and proven to meet the requirements.<sup>13</sup>

### 2.2 Instrumentation

Image acquisition of the array was performed with a smartphone (Apple iPhone 13). Pipettors were bought from

Eppendorf (Hamburg, Germany). A Costar 96-well EIA plate was purchased from Corning Inc. (Corning, NY, USA). BSA224S-CW electronic analytical balance was provided by Sartorius Scientific Instrument Co., LTD (Goettingen, Germany). BA-FZL6 automatic distiller was from Bayue Instrument Co., LTD (Changsha, China). L50-50-20 LED array light sources were purchased from Machine Vision Light Sources Co., LTD (Guangzhou, China).

### 2.3 Array response

Excess sulfur dioxide residues in food usually come from exogenous addition and sulfur-fumigation, *etc.* Generally, the residues of TCM and food raw material are mainly sulfur dioxide and sulfate substances after sulfur-fumigation. Residual sulfur dioxides are partially transformed to sulfites when encountering moisture from raw materials. Consequently, it is necessary to transform the remaining sulfur dioxide to sulfite through a hydration reaction before detection. Being very unstable, sulfite was protected by adding 1% formaldehyde and detected as soon as possible. The response points on the array were designed based on six specific color reactions that could occur with sulfite in conventional spectrophotometry.<sup>30–35</sup> These specific reactions were shown in Fig. S1.† The residual amount of sulfur dioxide represents the sum of the residual amounts of sulfur dioxide and sulfite in the samples.

### 2.4 Array analysis procedure

As shown in Fig. 1, the array analysis system consists of an array plate, an imaging system, and a personal computer. The supplementary light of the image is achieved through an LED array light source during image acquisition. The dimensions of each hole on the plate are 6 mm in diameter and 8 mm in height. The composition of the developed  $1 \times 6$  array was summarized in Table S1.† The workflow of the array was as follows: 200  $\mu\text{L}$  of each control solution was added to each well on the  $1 \times 6$  array (point-to-point, one reaction corresponds to one well on the array) according to Table S1† and the “before” images were obtained by smartphone. A series of work solutions with final concentrations of 0, 1, 3, 5, 7, 10, 50, 100, 500 and 1000  $\mu\text{g mL}^{-1}$  of sulfur dioxide were prepared (formulated with sodium sulfite). Similarly, work solutions were performed the same process as control solutions and the “after” images were acquired. Five replicates were performed separately. The correction of the image before and after the reaction and the removal of the background noise were performed through geometric correction and filtering. A normalized array image was generated by taking the spectral mean of the central region of each detected unit on the array as its spectral information code. The difference maps were achieved by subtracting the red, green and blue (RGB) values of the standard array images before and after. The RGB eigenvalues of each sensor unit were extracted and a  $3N$ -dimensional difference vector was generated, where  $N$  was the total number of sensor units (for a  $1 \times 6$  array, this difference vector was 18 dimensions). The total Euclidean distances (EDs) of the difference map were defined by the square root of the sums of the squares of the values of  $\Delta R$ ,  $\Delta G$  and  $\Delta B$ .



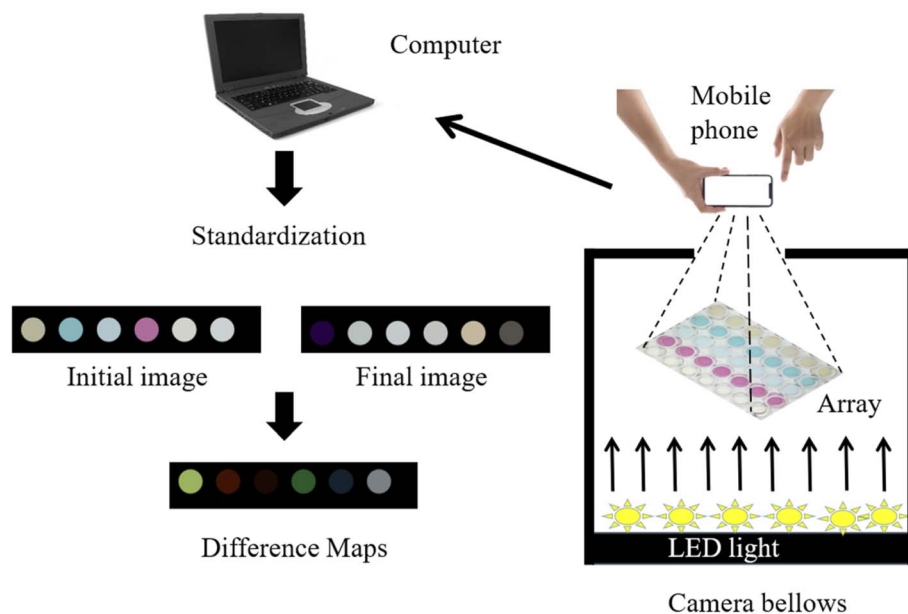


Fig. 1 Schematic diagram of the detection system, consisting of EIA plate-based  $1 \times 6$  colorimetric sensor array, smartphone-based colorimetric reader and personal computer-based image data analysis system. Before image acquisition, the array plate was placed on the white bottom plate of a self-made paper darkroom. Additional illumination was provided by a LED array light source when taking photos.

## 2.5 Analysis of real samples

1.00 g of *Fritillaria* was accurately weighed, crushed and transferred to 10 mL of PBS (0.01 M, pH 7.0). The supernatant of *Fritillaria* was collected after 2 min of shaking, 20 min of sonication, and 5 min of centrifugation at 12 000 rpm. The detection solution of *Fritillaria* (i.e., real sample) was prepared by adding sulfur dioxide to final concentrations of 30, 60 and 90  $\mu\text{g mL}^{-1}$ , respectively. The spiked real samples were analyzed by the array analysis procedure described above. Simultaneously, the determination of sulfur dioxide residue of real samples was performed by iodine titration, which is the standard method documented in GB 5009.34-2016.<sup>13</sup>

## 2.6 Data processing method and software

The image pretreatment and extraction of RGB values were performed using Matlab 2018a (Mathworks, Natick, MA, USA) and Photoshop CS4 (Adobe, San Jose, California, USA). All data statistics and diagram plotting were achieved based on SPSS 22.0 (IBM Corp., Armonk, N. Y., USA) and OriginPro 2021 Learning Edition (Origin Lab Corp., Northampton, MA, USA).

# 3. Results and discussion

## 3.1 Availability assessment of array

Based on the difference map of the array's six response points, a  $6 \times 3$ -dimensional dataset was obtained by extracting the color values of the RGB space, which could be seen as a nonlinear mapping from low-dimensional space to high-dimensional space. According to Cover's theorem, linear separability is more likely to be achieved in high dimensional space, which indicates that the proposed array has a high ability to

achieve differentiation.<sup>36</sup> Therefore, the as-fabricated array has a high-resolution ability in theory, which has the ability to achieve the discrimination of slight color differences.

Some components of real samples or reaction buffer solutions are likely to affect the response of the colorimetric sensor array. To evaluate the specificity of the colorimetric sensor array, several common components, including PBS, organic acids (e.g., vitamin C), amino acids (e.g., glutamic acid), sugars (e.g., glucose) and metal ions (e.g.,  $\text{K}^+$  and  $\text{Na}^+$ ), were designate as interferents and detected by the proposed array.<sup>37,38</sup> After adding high concentration interferents, there is no visible difference (i.e.,  $\Delta R$ ,  $\Delta G$  and  $\Delta B$  approach zero) through the comparison of the array response image before and after the reaction [Fig. S2(a)†]. Compared with the difference maps of interferents, the difference maps of the mixed group (interferents & sulfur dioxide) have obvious color changes, and the colors of difference maps between mixed groups are visually consistent [Fig. S2(b)†]. Moreover, the Euclidean distance of the difference maps had no significant difference between different interferents and between different mixed groups (Fig. 2). As shown in Fig. 3, there are visible differences between the difference maps of sulfur dioxide at different concentrations, and the results of multiple repeated trials show that there is no visible color change between the difference maps of the same concentration of sulfur dioxide. It indicates that the as-fabricated sensor exhibits a good availability and has a potential application for the detection of sulfur dioxide.

## 3.2 Qualitative analysis of sulfur dioxide by the array

To achieve a quantitative comparison of the color change of the array, the  $R$ ,  $G$  and  $B$  value was extracted and designated as feature information. A  $6 \times 3$ -dimensional dataset was obtained



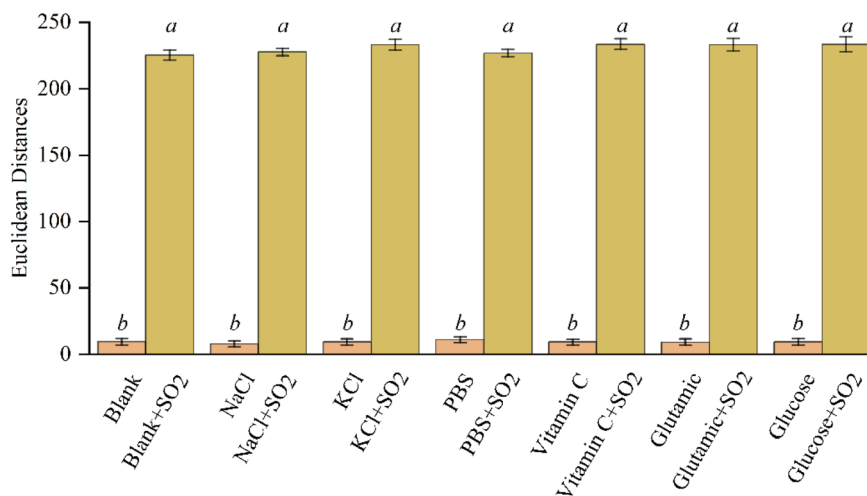


Fig. 2 Response of as-fabricated arrays to various potential interferents (final concentration of  $100 \mu\text{g mL}^{-1}$ ) in the absence (orange bars) and presence (yellow bars, final concentration of  $10 \mu\text{g mL}^{-1}$ ) of sulfur dioxide ( $\bar{X} \pm S$ ). The error bars show the standard deviation of quintuplicate experiments. Different italic letters in the figure indicate significant differences between groups at the 0.05 level using one-way ANOVA and Tukey's test.

and used for subsequent analysis. Because of the dispersive and nonlinear characteristics of image data, principal component analysis (PCA) and hierarchical cluster analysis (HCA) were respectively performed to explore the dispersion and aggregation tendencies of samples on account of the spatial structure of eigenvalues.<sup>39,40</sup>

The scatter plot of PCA shows that there is a trend toward clusters mainly along PC1 between sulfur dioxide and other components (Fig. S3†). The PC1 and PC2 explain 99.67% and 0.20% of total variance respectively, and the total cumulative variance reaches 99.87%. From Fig. 4, similar to PCA, the

diagram of HCA has the ability to completely separate interferent groups from mixed groups (contains interferents with a final concentration of  $100 \mu\text{g mL}^{-1}$  and sulfur dioxide with a final concentration of  $10 \mu\text{g mL}^{-1}$ ). Similar results were obtained by multiple random repeated sampling. In conclusion, it suggests that the array shows good specificity and selectivity.

To evaluate the response and discrimination of capacity to the amount of sulfur dioxide, a series of sample solutions of sulfur dioxide with final concentrations of 0, 10, 50, 100, 500 and  $1000 \mu\text{g mL}^{-1}$  were accurately prepared and measured through the array. As shown in Fig. S4,† the 2-dimensional plot

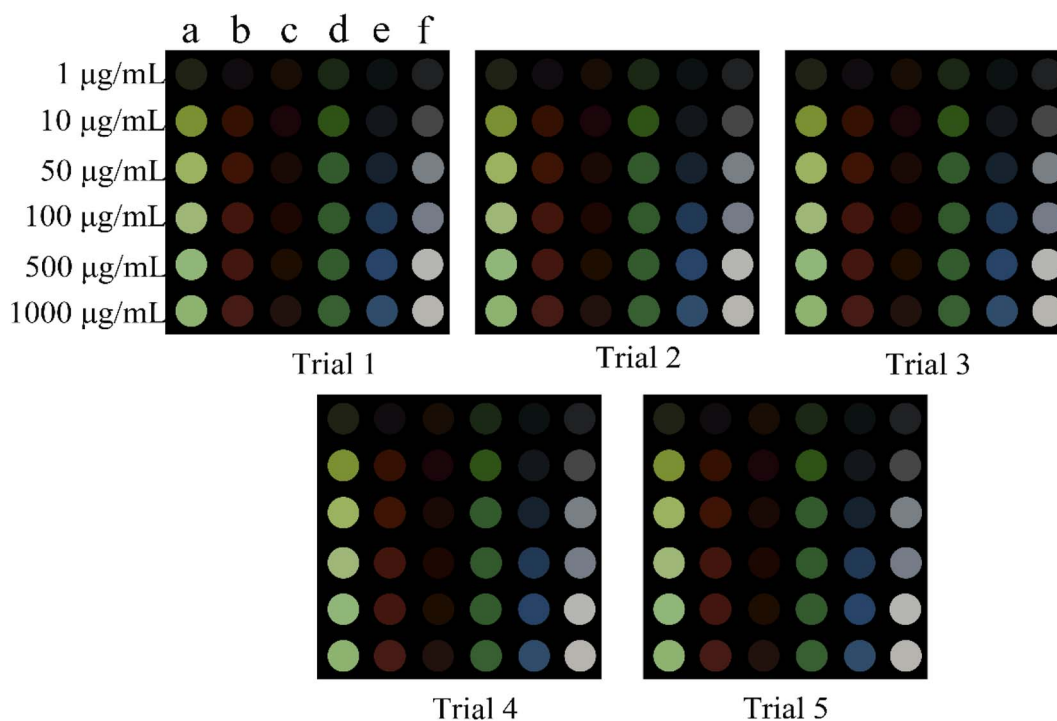


Fig. 3 Color difference maps of the array for sulfur dioxide at different concentrations. (a) Hydrochloric *para*-rosaniline, (b) brilliant green, (c) malachite green, (d) basic fuchsin, (e) OPA, (f) 1,10-phenanthroline and  $\text{Fe}^{3+}$ . All of the experiments were performed in quintuplicate.



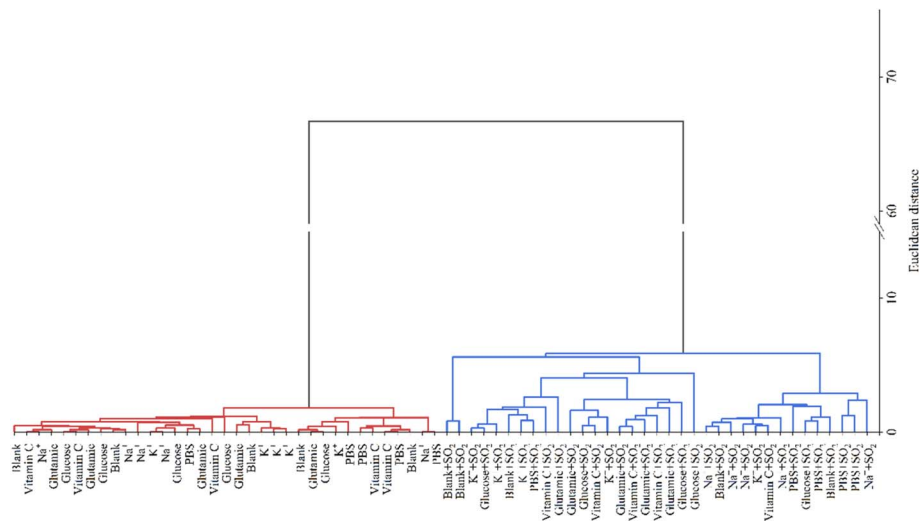


Fig. 4 Dendrogram of HCA of different interferents with and without sulfur dioxide. The final concentrations of interferents (e.g., blank,  $\text{Na}^+$ ,  $\text{K}^+$ , PBS, vitamin C, glutamic acid, glucose) and sulfur dioxide were  $100 \mu\text{g mL}^{-1}$  and  $10 \mu\text{g mL}^{-1}$ , respectively.

of PCA shows that the samples appear a clear cluster trend, just associated with seven concentrations of sulfur dioxide. The PC1 and PC2 explain 98.63% and 1.35% of total variance respectively and the total cumulative variance reaches 99.98%. From Fig. 5, the same result is also observed through the HCA diagram. Similar results were obtained with repeated sampling. It illustrates that the as-fabricated array has the ability to discriminate different amounts of sulfur dioxide. Predictably, combined with an automatic classifier based on a pattern recognition algorithm, it reaches a rapid screening of whether the sulfur dioxide residues of real samples exceed the standard.

As a common pattern recognition algorithm, the main idea of linear discriminant analysis (LDA) is as follows: the labeled training datasets are projected onto a straight line so that the data projection points of the same type of label are as close as possible and the data projection points of different types of labels are as far away as possible.<sup>41</sup> Then, the test data sets are projected to the same line, and the label type of the test data is determined according to the position of the projection point. Unlike PCA and

HCA, LDA takes full account of the label information of the sample and has the ability to achieve predictive analysis.

A series of sulfur dioxide with final concentrations of 1, 10, 50, 100, 500 and  $1000 \mu\text{g mL}^{-1}$  were prepared, respectively. Five samples and two samples were randomly selected from each concentration of sulfur dioxide and designated as training samples and test samples respectively. Therefore, thirty training datasets (RGB values) and twelve testing datasets (RGB values) were obtained by the as-fabricated array. As shown in Fig. 6, the test samples are successfully assigned to the training sample groups according to the different concentrations of sulfur dioxide. The prediction performance of LDA is consistent after multiple random sampling.

### 3.3 Quantitative analysis of sulfur dioxide by the array

The relationship between the color changes of the array [defined by the total Euclidean distances (EDs)] and the concentrations of

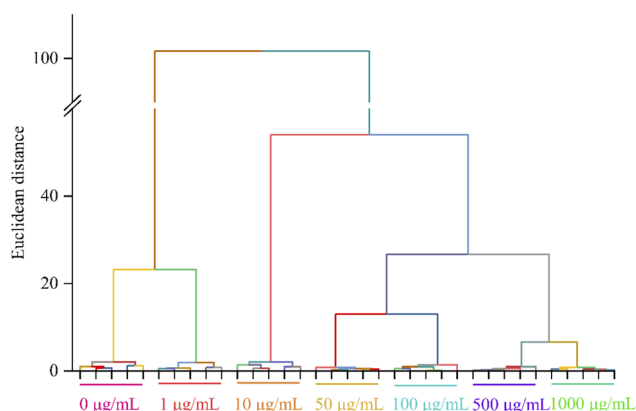


Fig. 5 Cluster diagram of the response of different sulfur dioxide concentrations. All of the experiments were performed in quintuplicate.

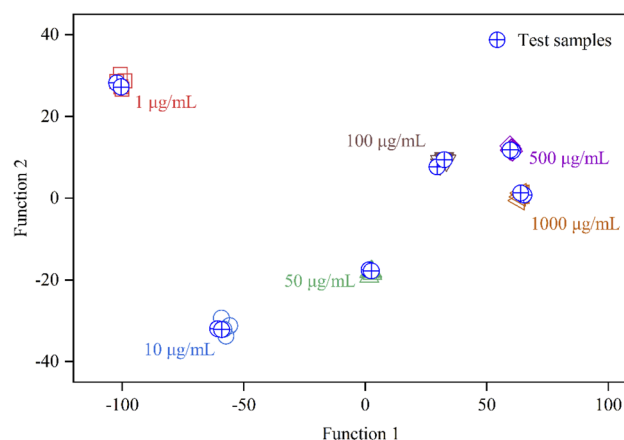


Fig. 6 Discriminant diagram of response to different sulfur dioxide concentrations. Five samples and two samples were randomly selected from each concentration of sulfur dioxide, and there were thirty training sets and twelve testing sets.



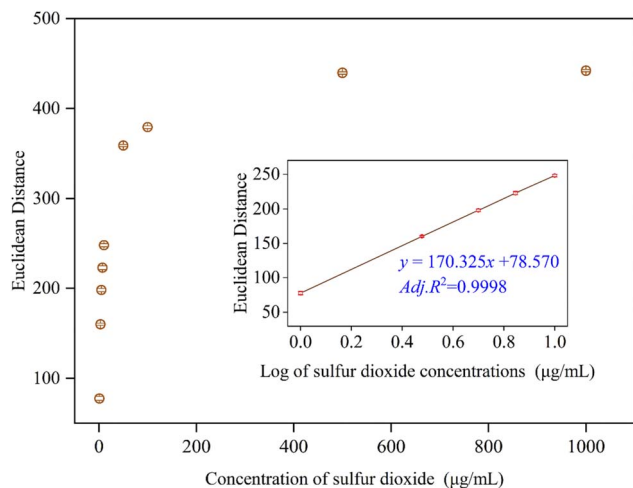


Fig. 7 A trend of total Euclidean distance (EDs) of the array and different concentration of sulfur dioxide ( $\bar{X} \pm S$ ). Inset: the linear relationship in the logarithm of sulfur dioxide concentration from 1 to 10  $\mu\text{g mL}^{-1}$ . Error bars shows five parallel measurements.

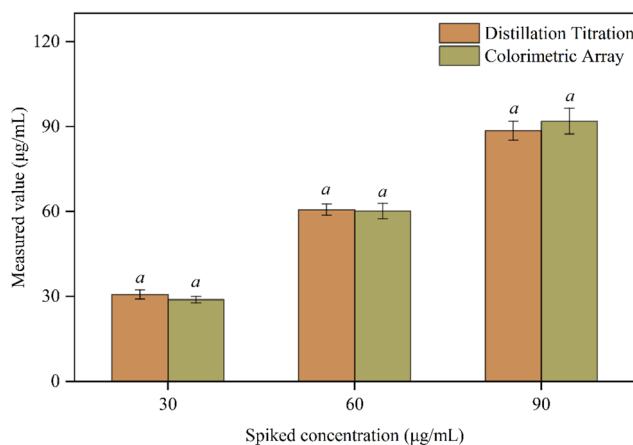


Fig. 8 Comparison of colorimetric sensor array and distillation titration for the detection of sulfur dioxide ( $\bar{X} \pm S$ ). The same lowercase letter indicates that the test results of the two methods are not significantly different at the 0.05 level by paired  $t$ -test.

sulfur dioxide was observed by scatter plot. As shown in Fig. 7, EDs versus sulfur dioxide concentration shows a linear range of 1 to 1000  $\mu\text{g mL}^{-1}$ , and a good linearity range from 1 to 10  $\mu\text{g mL}^{-1}$  (inset of Fig. 7). It indicates the as-fabricated colorimetric sensor array has the potential to achieve the quantitative analysis of

sulfur dioxide through the corresponding fitting curve. A LOD of  $0.406 \mu\text{g mL}^{-1}$  calculated by the  $3\sigma$  rule was reached through the literature.<sup>42</sup> From Chinese National Standard GB 5009.34-2016,<sup>13</sup> the limits of detection (LOD) of sulfur dioxide are  $1.5 \mu\text{g mL}^{-1}$  by distillation titration. In addition, by comparison with the detection limit of conventional detection methods (Table S2†). It demonstrates that the as-fabricated colorimetric sensor array has an excellent linear region at low concentration range of sulfur dioxide and a low LOD.

### 3.4 Comparison of detection of sulfur dioxide in real samples by the array and distillation titration

Three real samples (*Fritillaria*) extracts containing the final concentration of 30, 60, and 90  $\mu\text{g mL}^{-1}$  of sulfur dioxide were prepared and tested simultaneously by the proposed array and distillation titration according to Chinese National Standard GB 5009.34-2016.<sup>13</sup> The difference maps of spiked samples show specific color fingerprints during repeated experiments (Fig. S5†). From Fig. 8, there is no significant difference between the test results of the array and distillation titration by paired  $t$ -tests. It indicates that the as-fabricated array shows a potential application for the detection of sulfur dioxide. Although the distillation titration is simple to operate, the analysis is time-consuming and lead-containing detection reagents have the risk of environmental pollution.<sup>43</sup> Due to simple operation, less time-consuming, good specificity and relatively low risk of environmental pollution, the as-fabricated array shows potential to replace distillation titration for sulfur dioxide detection.

### 3.5 Evaluation of accuracy, precision and repeatability

Extracts of *Fritillaria* with a final concentration of sulfur dioxide of 30, 60 and 90  $\mu\text{g mL}^{-1}$  were prepared and determined quantitatively by the array and fitting curve. Samples of the same concentration were prepared in sextuplicate, and then there were a total of eighteen spiked samples. Each spiked sample was measured once to assess accuracy and precision, and a spiked sample was randomly selected from different concentration groups and measured continuously for six times to assess reproducibility. Accuracy was expressed as mean value  $\pm$  standard deviation (STD/SD) and relative recovery (RR). Precision (intra-assay) and reproducibility were evaluated via relative standard deviations (RSD). As can be seen from Table 1, the results show that the recovery and RSD value of sulfur dioxide is in the range of 97–103% and 2.16–4.97%, respectively. It states clearly that the array develops a cost-effective and

Table 1 The results of accuracy, precision, and repeatability<sup>a</sup>

Spiked sulfur dioxide concentration ( $\mu\text{g mL}^{-1}$ )	Accuracy			
	Mean $\pm$ STD ( $\mu\text{g mL}^{-1}$ )	Recover rate, %	Precision RSD, %	Repeatability RSD, %
30	$28.86 \pm 1.14$	93.06–100.43	3.95	4.32
60	$60.10 \pm 2.75$	95.93–105.05	4.58	3.27
90	$91.93 \pm 4.57$	97.06–107.21	4.97	2.16

<sup>a</sup> Note: STD, standard deviation; RSD, relative standard deviation.



potential method for the quantitative analysis of sulfur dioxide in real sample with the good performance of accuracy, precision and reproducibility.

## 4. Conclusions

Excess sulfur dioxide residues in some food or TCM on the market are possibly added by sulfur-fumigation. The main residual components after sulfur-fumigation are divided into sulfur dioxide and sulfites, and sulfur dioxide is easily transformed to sulfites. Here sulfite was chosen as the detection target for the proposed array reaction.

A simple, inexpensive and practical colorimetric sensor array based on commercially available reagents and six specific chemical reactions for the detection and discrimination of sulfur dioxide was developed in this work. The results of PCA and HCA reveal that the sensor array can achieve the identification and differentiation of sulfur dioxide from other potentially interferents. Moreover, semi-quantitative and quantitative detection of sulfur dioxide also has the capacity to be achieved through corresponding pattern recognition and curve fitting. And crucially, the as-fabricated array also shows potential applications for the detection of sulfur dioxide in real samples and exhibits good accuracy, precision and repeatability.

## Conflicts of interest

All authors declare that we have no conflict of interest.

## Acknowledgements

This work was financially supported by Science and Technology Bureau of Wanzhou, Chongqing, China (No. WZSTC20210313), National Innovation and Entrepreneurship Training Program for College Students (202010643003), Natural Science Foundation of Chongqing (No. cstc2021jcyj-msxmX0924) and sharing fund of Engineering Technology Research Center for the Development and Utilization of Characteristic Biological Resources in Northeast Chongqing.

## References

- 1 X. Jiang, L. F. Huang, S. H. Zheng and S. L. Chen, *Phytomedicine*, 2013, **20**, 97–105.
- 2 A. Vehapoğlu, E. Çakır, S. Uzun, F. Çalım Ö and H. Yazan, *Turkish archives of otorhinolaryngology*, 2020, **58**, 286–288.
- 3 E. I. Zaki, A. R. El-Mahdy, H. M. El-Gamal and A. S. El-Seedy, *Cell. Mol. Biol.*, 2021, **67**, 66–75.
- 4 J. Jiang, S. Xiao, S. Yan, J. Zhang and X. Xu, *J. Ethnopharmacol.*, 2020, **249**, 112377.
- 5 J. Y. Zhan, P. Yao, C. W. Bi, K. Y. Zheng, W. L. Zhang, J. P. Chen, T. T. Dong, Z. R. Su and K. W. Tsim, *Phytomedicine*, 2014, **21**, 1318–1324.
- 6 Y. Huang, H. Zhang, B. Lv, C. Tang, J. Du and H. Jin, *Antioxid. Redox Signaling*, 2022, **36**, 256–274.
- 7 T. D'Amore, A. Di Taranto, G. Berardi, V. Vita, G. Marchesani, A. E. Chiaravalle and M. Iammarino, *Compr. Rev. Food Sci. Food Saf.*, 2020, **19**, 2701–2720.
- 8 H. Feng, J. Liu, A. Qaitoon, Q. Meng, Y. Sultanbawa, Z. Zhang, Z. P. Xu and R. Zhang, *TrAC, Trends Anal. Chem.*, 2021, **136**, 116199.
- 9 M. Kong, H. H. Liu, J. Wu, M. Q. Shen, Z. G. Wang, S. M. Duan, Y. B. Zhang, H. Zhu and S. L. Li, *J. Ethnopharmacol.*, 2018, **212**, 95–105.
- 10 C. Y. Wu, M. Kong, W. Zhang, F. Long, J. Zhou, S. S. Zhou, J. D. Xu, J. Xu and S. L. Li, *Food Chem.*, 2018, **239**, 953–963.
- 11 Chinese Pharmacopoeia Commission, *Pharmacopoeia of the People's Republic of China*, Chinese Medical Science and Technology Press, Beijing, China, 2005.
- 12 Chinese Pharmacopoeia Commission, *Pharmacopoeia of the People's Republic of China*, Chinese Medical Science and Technology Press, Beijing, China, 2010.
- 13 National Health and Family Planning Commission of China, *National Food Safety Standard-Determination of Sulfur Dioxide in Foodstuffs GB 5009.34-2016*, Standards Press of China, Beijing, China, 2017.
- 14 D. Han, T. Luo, L. Zhang, J. Wu, H. Wu, Z. Wu, J. Li, J. Wang and X. Pan, *Food Sci. Nutr.*, 2020, **8**, 2827–2838.
- 15 A. Skok, Y. Bazel and A. Vishnikin, *J. Sulfur Chem.*, 2022, **43**, 443–471.
- 16 L. A. N. Dayao, C. C. Liu, S. Y. Hsu, L. L. Tayo, W. J. Ju and L. M. Fu, *Anal. Chim. Acta*, 2019, **1071**, 44–52.
- 17 Q. Hu, R. Guo, L. Zhang, Q. Liu, S. Cai and W. Lin, *Luminescence*, 2021, **36**, 1006–1012.
- 18 X. Bao, X. Cao, Y. Yuan, B. Zhou and C. Huo, *J. Agric. Food Chem.*, 2021, **69**, 4903–4910.
- 19 C. Kang, D. Zhao, L. Kang, S. Wang, C. Lv, L. Zhou, J. Y. Jiang, W. Yang, J. Li, L. Q. Huang and L. Guo, *Front. Plant Sci.*, 2018, **9**, 790.
- 20 B. Lajin and W. Goessler, *Anal. Chim. Acta*, 2019, **1092**, 1–8.
- 21 H. Park, H. D. Lim, H.-K. Lim, W. M. Seong, S. Moon, Y. Ko, B. Lee, Y. Bae, H. Kim and K. Kang, *Nat. Commun.*, 2017, **8**, 14989.
- 22 Y. Lv, R. Wu, K. Feng, J. Li, Q. Mao, H. Yuan, H. Shen, X. Chai and L. Li, *J. Nanobiotechnol.*, 2017, **15**, 35.
- 23 H. Yan, P. H. Li, G. S. Zhou, Y. J. Wang, B. H. Bao, Q. N. Wu and S. L. Huang, *Food Chem.*, 2021, **341**, 128241.
- 24 N. A. Rakow and K. S. Suslick, *Nature*, 2000, **406**, 710–713.
- 25 M. R. Mirghafouri, S. Abbasi-Moayed, F. Ghasemi and M. R. Hormozi-Nezhad, *Anal. Methods*, 2020, **12**, 5877–5884.
- 26 Y. Zhu, J. Wu, L. Han, X. Wang, W. Li, H. Guo and H. Wei, *Anal. Chem.*, 2020, **92**, 7444–7452.
- 27 L. Yan-Qi and F. Liang, *Chin. J. Anal. Chem.*, 2020, **48**, 1448–1457.
- 28 S. Sun, S. Qian, J. Zheng, Z. Li and H. Lin, *Analyst*, 2020, **145**, 6968–6973.
- 29 S. Qian, Y. Wang and H. Lin, *Talanta*, 2018, **181**, 305–310.
- 30 Z. Ma, L. Gu, L. Zeng and J. Li, *Sci. Technol. Food Ind.*, 2012, **33**, 72–74.
- 31 S. K. Goyal, *J. Environ. Monit.*, 2001, **3**, 666–670.
- 32 X. Bao, X. Cao, Y. Yuan, B. Zhou and C. Huo, *Journal of Agricultural*, 2021, **69**, 4903–4910.



- 33 N. Huo, D. Li, S. Zheng and W. Deng, *Chem. Eng. J.*, 2022, **432**, 134317.
- 34 Y. Xiong, Q. Wang, X. Li, S. Fang and M. Duan, *Chromatographia*, 2018, **81**, 1003–1011.
- 35 A. Shahvar, M. Saraji, H. Gordan and D. Shamsaei, *Talanta*, 2019, **197**, 578–583.
- 36 T. M. Cover, *IEEE Trans. Electron. Comput.*, 1965, **3**, 326–334.
- 37 M. Sundhoro, S. R. Agnihotra, B. Amberger, K. Augustus, N. D. Khan, A. Barnes, J. BelBruno and L. Mendecki, *Food Chem.*, 2021, **344**, 128648.
- 38 M. Bener, F. B. Şen and R. Apak, *Spectrochim. Acta, Part A*, 2020, **226**, 117643.
- 39 D. Cozzolino, A. Power and J. Chapman, *Food Anal. Methods*, 2019, **12**, 2469–2473.
- 40 D. Granato, J. S. Santos, G. B. Escher, B. L. Ferreira and R. M. Maggio, *Trends in Food Science Technology*, 2018, **72**, 83–90.
- 41 H. Ma, J. Yan, Y. Li, C. Zhang and H. Lin, *Acta Geophys.*, 2019, **67**, 109–121.
- 42 Y. H. Lin and W. L. Tseng, *Chem. Commun.*, 2009, **43**, 6619–6620.
- 43 B. Lajin and W. Goessler, *Anal. Chim. Acta*, 2019, **1092**, 1–8.

